



Development of turbulent scheme in the FLEXPART-AROME v1.2.1 Lagrangian particle dispersion model

Bert Verreyken^{1,2,3}, Jérôme Brioude¹, and Stéphanie Evan¹

¹Laboratoire de l'Atmosphère et des Cyclones, UMR 8105 CNRS, University of Réunion Island, Reunion Island, France

²Belgian Institute for Space Aeronomy, Ringlaan 3, B-1180 Brussels, Belgium

³Ghent University, Department of Chemistry, Krijgslaan 281 - S3, B-9000 Ghent, Belgium

Correspondence: B.Verreyken (bert.verreyken@aeronomie.be)

Abstract. The FLEXPARTible PARTicle dispersion model FLEXPART, first released in 1998, is a Lagrangian particle dispersion model developed to simulate atmospheric transport over large and meso-scale distances. Due to FLEXPART's success and its open source nature, different limited area model versions of FLEXPART were released making it possible to run FLEXPART simulations by ingesting WRF (Weather Research Forecasting model) or MM5 (meso-scale community model maintained by Penn State university) meteorological fields on top of the ECMWF (European Centre for Medium-Range Weather Forecasts) and GFS (Global Forecast System) meteorological fields. Here, we present a new FLEXPART limited area model that is compatible with the AROME mesoscale meteorological forecast model (the Applications of Research to Operations at Meso-scale model)¹. FLEXPART-AROME was originally developed to study meso-scale transport around La Réunion, a small volcanic island in the South West Indian Ocean with a complex orographic structure which is not well represented in current global operational models. The AROME vertical hybrid sigma grid is projected on the Cartesian terrain following FLEXPART grid. We present new turbulent modes in FLEXPART-AROME. They differ from each other by: dimensionality, mixing length parameterisation, turbulent transport constraint interpretation and a novel time-step configuration. Performances of new turbulent modes are compared to the ones in FLEXPART-WRF by testing the conservation of well-mixedness by turbulence, the dispersion of a point release at the surface and the marine boundary layer evolution around Reunion island. An adaptive time step for the vertical turbulent motions has been implemented to improve conservation of well-mixedness in the model.

1 Introduction

Atmospheric transport models are divided into Eulerian and Lagrangian transport models. Eulerian models represent the atmosphere in a grid with mass being exchanged between grid cells. They are especially useful to model chemical interactions in the atmosphere. However, Eulerian models are unable to maintain the shape of narrow plumes due to numerical diffusion in their advection scheme. Lagrangian models on the other hand describe the evolution of air masses in 3D wind fields obtained from

¹Applications de la Recherche à l'Opérationnel à Méso-Echelle



a numerical weather prediction (NWP) model allowing precise modelling of atmospheric tracers released from point-sources. Uncertainties in Lagrangian models are limited and originate from naive linear temporal and spatial interpolation from the 3D meteorological fields of the NWP model (Stohl et al., 1995). Lagrangian particle diffusion models (LPDM) such as FLEXPART represent an air mass by a large amount of infinitesimally small air parcels, also called particles, into the atmosphere.

5 Each individual particle is advected along the resolved wind fields with a turbulent diffusion superimposed. (Zannetti, 1990)

LPDMs are used in a variety of atmospheric studies such as source apportionment of chemical compounds (Gentner et al., 2014; Warneke et al.), studying atmospheric water vapor transport (Bertò et al., 2004; D'Aulerio et al., 2005; James et al., 2008), characterising deep stratospheric intrusions (Brioude et al., 2007; Akritidis et al., 2012), as well as hazard preparedness exercises (Stohl, 2013).

10 Pisso et al. (2019) describe the FLEXPART offline transport model. The latest release ingests meteorological data from the ECMWF and GFS global model. Several limited area models have already been developed allowing particle transport in higher resolved grids with the possibility to better represent the mesoscale phenomena in the atmosphere.

The AROME mesoscale forecast model has been the operation weather forecasting model at Météo France since 2008. It is designed for fine-scale modelling with grid sizes ranging from 0.5 to 2.5 km. AROME is developed by combining efforts of

15 the French Meso-NH research model community and the ALADIN consortium². Since 2015, the French metropolitan area is covered by a 1.3 km horizontally resolved grid in a Lambert conformal projection which results not only in a more realistic representation of topologically induced physical phenomena but also allows for a fine scale variation in surface types impacting for instance the sensible heat flux at the surface (MétéoFrance). FLEXPART-AROME was developed by the LACy laboratory to model particle transport around La Réunion, a french overseas territory which is covered by an AROME grid in the South-

20 West Indian Ocean (AROME-SWIO) with 2.5x2.5 km² horizontal resolution in a Lambert Conformal projection. With its 90 vertical hybrid sigma levels it reaches an atmospheric altitude of about 24 km above sea level. A provisional version of FLEXPART-AROME was successfully used in the 2015 STRAP campaign to forecast transport of a volcanic plume on the Island (Tulet et al., 2017).

FLEXPART-AROME is based on the FLEXPART-WRF code which is able to use the Lambert Conformal projections in the

25 horizontal coordinate. The hybrid sigma levels are projected on Cartesian terrain-following vertical levels used by FLEXPART. To simulate turbulence induced by the complex orographic structure of the volcanic island of La Réunion and by shallow convection, we built on the turbulent modes implemented in FLEXPART-WRF by ingesting the 3D turbulent kinetic energy (TKE) field from the NWP in FLEXPART in order to harmonise turbulent motions between both.

2 Turbulent inconsistency between NWP and LDPM

30 Incoherent turbulent representations may introduce unrealistic tracer transport features. For instance, if the planetary boundary layer height (PBL) is overestimated in the transport model, tracers will be advected along stronger free tropospheric (FT) winds

²The ALADIN consortium contains the Algerian, Austrian, Belgian, Bulgarian, Croatian, Czech Republic, French, Hungarian, Moroccan, Polish, Portuguese, Romanian, Slovakian, Slovenian, Tunisian and Turkish weather services.



with a different direction. If the reverse is true and the PBL height is underestimated a passive tracer released at the surface will be well-mixed over a smaller vertical range, overestimating tracer concentrations in the boundary layer. The FLEXPART Lagrangian particle dispersion model uses a turbulent parameterisation independent of the NWP model. It was proposed by Hanna (1982), developed and validated for meso-scale models. The PBL height is calculated by the method proposed by

5 Voegeleang and Holtslag (1996). FLEXPART-WRF implemented turbulent modes using the 3D TKE fields. However, they were reported to violate the well-mixedness condition by Thomson (1987), which states that turbulent behaviour cannot change an initially well-mixed atmosphere. To resolve this we applied the method proposed by Thomson et al. (1997), successfully used in the Stochastic Time-Inverted Lagrangian Transport (STILT) model (Lin et al., 2003), to constrain particle transport keeping with the well-mixed criterion. When comparing the PBL localisation in FLEXPART with robust estimates based on

10 the temperature (θ_v) profile in AROME (fig 1). Above sea FLEXPART seems to systematically underestimate the PBL top location while in a mountainous region the reverse is true. When using TKE fields in AROME to check the depth of the turbulent layer starting from the surface, the comparison is less straightforward. Since turbulent kinetic energy in AROME includes energy from shallow convection and convective clouds, clouds situated at the PBL top allow surface tracers to cross the PBL top into the free troposphere. This last is a major difference between the novel TKE formalism in FLEXPART-AROME

15 and FLEXPART turbulence. In FLEXPART, mass transport between PBL and the FT is only possible by resolved winds and particles reaching the PBL top by turbulent motions are reflected. In FLEXPART-AROME we do not define the PBL region and only look at turbulent versus non-turbulent regions. Convective clouds reaching and crossing the PBL top are simply treated as turbulent regions promoting mixing not explicitly represented in FLEXPART. This is clearly illustrated in the vertical profiles of θ_v and TKE, shown in figure 2. It is also clear in this figure that due to the arbitrary nature of the tke limit used in diagnosing

20 turbulent layer depth in AROME, small variations in bridging the turbulence between PBL and clouds can cause what seems erratic behaviour in the diagnosed turbulent layer depth. On average, FLEXPART overestimates the PBL top over land by 133 m while over sea it is underestimated by 158 m (a difference in PBL depth of +25% and -61% respectively) over the 9 day period we randomly selected.

3 Turbulent scheme development

25 Turbulence in FLEXPART and FLEXPART-AROME is assumed Gaussian and parametrised using a Markov process to solve the Langevin equation. For a discrete time step implementation this results in:

$$\left(\frac{w}{\sigma_w}\right)_{k+1} = r_w \left(\frac{w}{\sigma_w}\right)_k + \sqrt{1+r_w^2} \zeta + \frac{\partial \sigma_w}{\partial z} \tau_{L_w} (1-r_w) + \frac{\sigma_w}{\rho} \frac{\partial \rho}{\partial z} \tau_{L_w} (1-r_w), \quad (1)$$

where w is the vertical wind component of the turbulent motion, L_w the turbulent mixing length, τ_{L_w} the Lagrangian time scale for the vertical autocorrelation, σ_w the vertical turbulent velocity distribution width, ρ the air density, z the altitude,

30 $r_w = \exp -dt/\tau_{L_w}$ the autocorrelation of the vertical wind and ζ a normally distributed random number with mean zero and unit standard deviation. The subscript k and $k+1$ refer to subsequent times separated by dt . The first two terms on the right

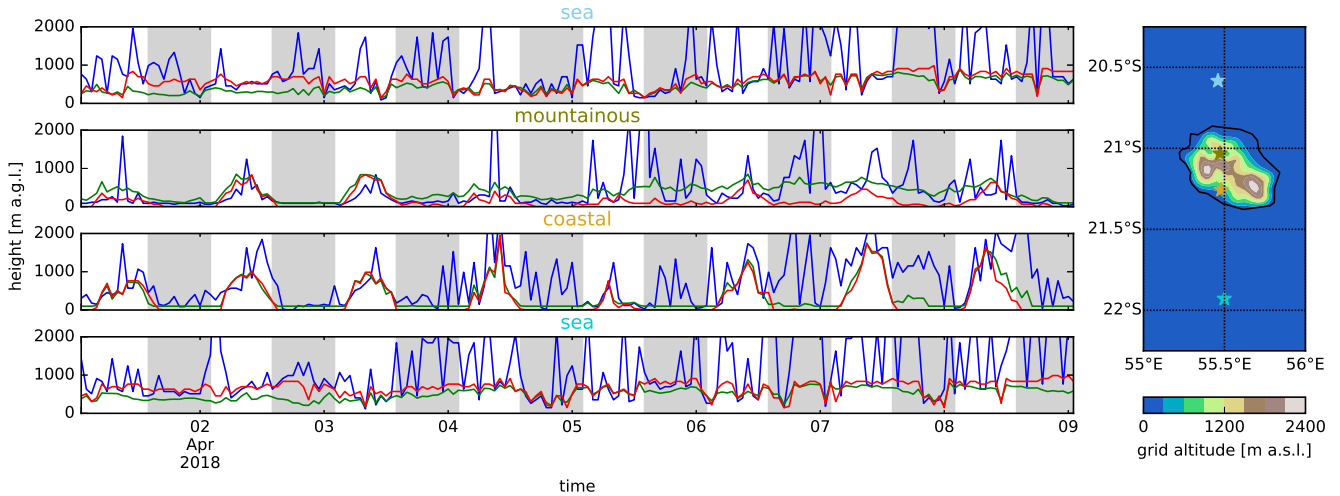


Figure 1. PBL top time evolution according to FLEXPART (green) and inferred from the θ_v profiles in AROME (red). Blue represent the turbulent layer from the surface up including turbulent clouds resolved in the tke profile from AROME. Shaded background indicate local night time. Based on TKE profiles, the turbulent region at the surface is deeper than the PBL top suggests. Differences between parameterisations cause over- or under mixing of surface tracers inducing density variations between independent models.

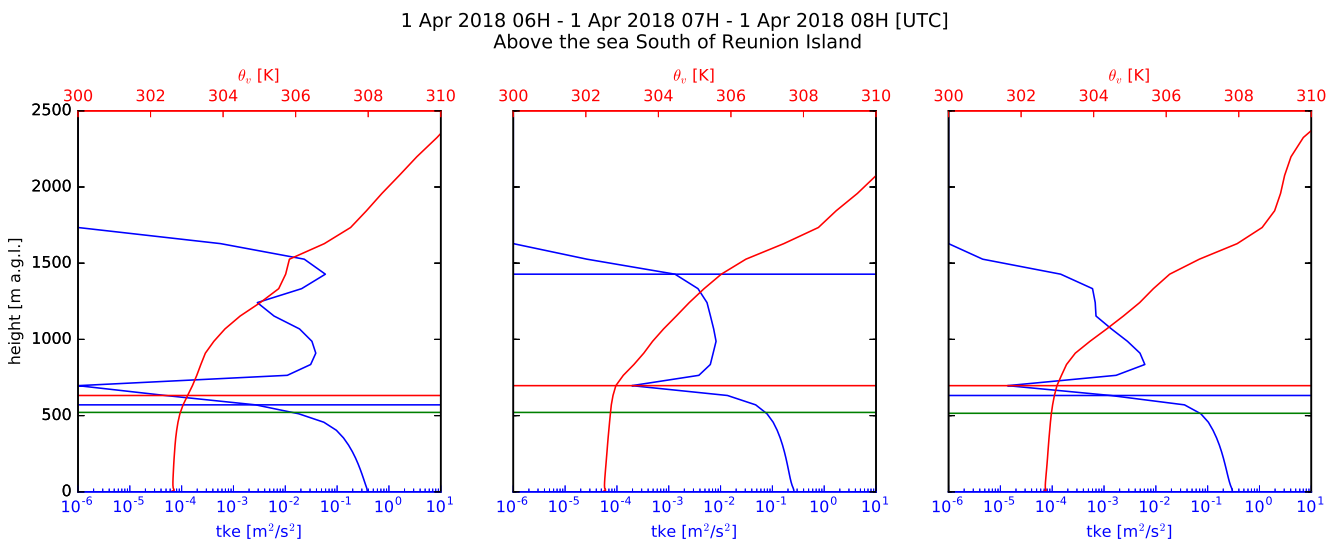


Figure 2. Vertical cross sections for three subsequent hours above the sea South of Reunion Island. Red shows the θ_v profile, blue shows the TKE profile. Horizontal lines correspond with PBL heights from FLEXPART and θ_v , shown in green and red respectively. The blue horizontal line characterises the turbulent layer from the surface including convective clouds based on the TKE profile. The turbulent layer top is defined as the lower bound of the model layer where the TKE drops below $1.e-4 \text{ m}^2/\text{s}^2$. A fast inclination of θ_v indicates the beginning of the FT, we found that the altitude where θ_v is 0.5K above its surface value robustly corresponds with the PBL top.



Table 1. Different turbulent options introduced in FLEXPART-AROME and their configuration.

TURB_OPTION		Bottom-up		Top-down	
		1D	3D	1D	3D
Step TKE	DELTA	10	15	20	25
	BL89	11	16	21	26
	DEARDORFF	12	17	22	27
SDA	DELTA	110	115	120	125
	BL89	111	116	121	126
	DEARDORFF	112	117	122	127

hand side represent the native autocorrelated turbulent velocity behaviour. The third and fourth terms represent drift and density corrections respectively.(Stohl et al., 2005)

To determine τ_{L_w} and σ_w , FLEXPART-WRF has four modes defined by the TURB_OPTION input parameter introduced by Brioude et al. (2013):

- 5 – TURB_OPTION = 0: Turbulent velocities are set to zero.
- TURB_OPTION = 1: Turbulence is computed using the standard FLEXPART configuration using the parametrisation proposed by Hanna (1982).
- TURB_OPTION = 2: A hybrid configuration combining TKE fields from WRF and FLEXPART parametrisation. Surface-layer scaling and local stability with the Hanna scheme determine the 3D partitioning of the turbulent kinetic energy.
- 10 – TURB_OPTION = 3: Turbulent motions are characterised directly by the TKE field from WRF and 3D partitioning is based on balancing production and dissipation of turbulent energy.

Brioude et al. (2013) reported spurious accumulation when using modes where TKE fields from the WRF are taken to characterise the turbulence.

- 15 In the FLEXPART-AROME code, the density and drift correction is set to zero and replaced by using Thomson interfaces. The turbulent configurations are also extended by 24 modes summarised in table 1. We separated the new options according to the characteristics of each mode, these characteristics will be discussed in greater detail below. The user has a choice in parametrisations for mixing length, the time-loop configuration and the partitioning of TKE. Turbulent motions can be restricted to the vertical axis, as it is in AROME-SWIO, or partitioned in 3D using the diagnostic equations from Meso-NH
- 20 mesoscale model.



3.1 Thomson's approach

Thomson et al. (1997) discussed the transport of particles through discrete interfaces in a random walk dispersion model. To conserve a well-mixed profile in a turbulent system with discrete TKE steps, particle transport is constrained between different TKE regions. By imposing a net zero mass-flux at TKE interfaces in a well-mixed system and assuming maximal mixing, particles attempting to cross an interface have a probability α of reflection. This probability is proportional to the ratio of Gaussian turbulent velocity distribution widths. Lin et al. (2003) introduced a correction to this probability due to density variations. In FLEXPART-AROME, this correction was not implemented as it is taken into account when solving the Langevin equation (Stohl and Thomson, 1999).

In FLEXPART-AROME, two possible interpretations of this principle have been implemented. The first considers each displacement a small discontinuity while the second arises from the grid definition of the FLEXPART-AROME model. In the small discontinuity approximation (SDA), turbulent kinetic energy is interpolated in time and space for both the initial, and the final position of a time step dt . The particle is supposed to cross an imaginary interface at the middle of its trajectory. The probability of crossing is given by $\alpha = \frac{\sigma_f}{\sigma_i}$, where σ_i and σ_f represent the widths of the turbulent velocity distributions at the initial and final position respectively. The difference between both interpretations is visualised in figure 3. Alternatively, one can consider the FLEXPART grid as a stack of homogeneously turbulent cells. The vertical cell-boundaries are discrete TKE interfaces and particles attempting to cross into an neighbouring cell are reflected with a probability α . In this mode (Step TKE), particles moving a distance dz are checked to see if they cross the cell boundary. If so, the time step is split up in the time it takes for the particle to get to the boundary (dt_1), and the remaining time ($dt_2 = dt - dt_1$). When a particle crosses the boundary, the turbulent velocity is recalculated to be consistent with the new local turbulence.

3.2 Particle time loop

FLEXPART particles are categorised in below PBL and above PBL. Above the PBL, particles are advanced in one user defined model synchronisation (LSYNC) time step. Below PBL the positions are updated along a leap-frog between turbulent transport and resolved wind fields. The Δt timestep is determined by the atmospheric stability and the user defined input parameter CTL. Vertical turbulent transport is handled in a second IFINE time loop with a time step $dt = \frac{\Delta t}{IFINE}$, where IFINE is a user defined input parameter.

A major difference between the FLEXPART-AROME and other FLEXPART versions is this discrimination at the PBL top. By direct use of TKE field from the NWP model we don't characterise the PBL height explicitly and all particles are put through the time loops. In very low turbulent regions, σ_w is low which naturally results in longer time steps:

$$\Delta t = \frac{\tau_w}{CTL}, \quad \tau_w = \frac{L_w}{\sigma_w}. \quad (2)$$

When large steps in TKE are made by a particle, Δt can change significantly. In the traditional FLEXPART code, this mismatch in time step carries through the remaining IFINE loops resulting in incorrect representation of the turbulent state in the new turbulent modes. In FLEXPART-AROME bottom-up time loop is implemented where Δt is accumulated during

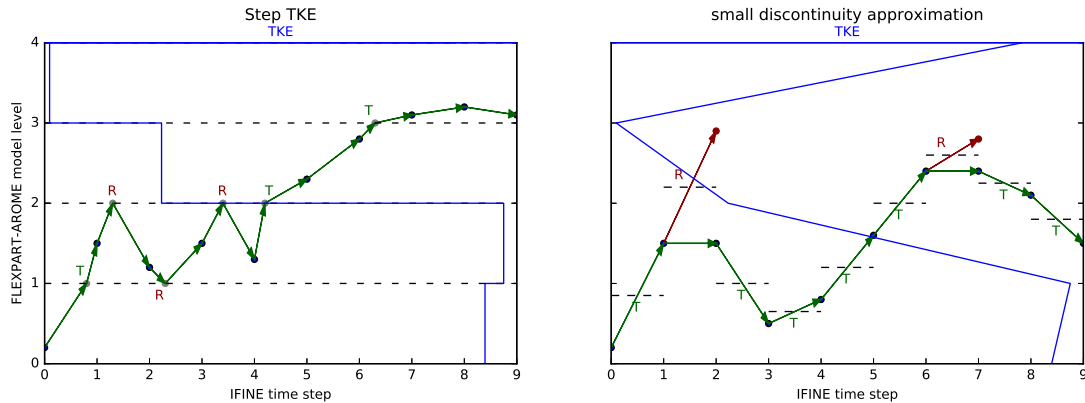


Figure 3. Illustrative difference between Step TKE configuration and SDA. Dashed lines represent TKE interfaces, in the Step TKE configuration they are fixed with homogeneous TKE regions inbetween, the SDA interpolates TKE to the particle position and initialises an imaginary temporary TKE interface halfway the particles trajectory each step. Every time the particle tries to cross an interface we evaluate the probability of crossing and the particle will be either transmitted through (T), or reflected (R) at the interface. The Step TKE configuration updates particle positions to the boundary before computing the probability of crossing (grey points), when particles are transmitted, their turbulent velocity is adapted to the new model layer. The SDA configuration uses a virtual position which becomes reality upon transmission or which is never realised upon reflection (red points).

IFINE dt time steps where:

$$dt = \frac{\tau_w}{CTL \times IFINE}. \quad (3)$$

In each IFINE loop, this dt is recalculated resulting in an adaptive time step in the bottom-up time loop configuration. Individual particles evaluate their local time step after each displacement and tell the algorithm how long it took them to finish IFINE steps. This in contrast to the top-down FLEXPART implementation where dt is constant throughout a precomputed Δt time step.

3.3 Turbulent mixing length

There are currently three parametrisations for the turbulent mixing length available in FLEXPART-AROME. The first is based on the grid size (DELTA). It is commonly used as the characteristic length scale of sub-grid eddies and is justified when the grid size falls into the inertial subrange of the turbulent flow and is recommended when the NWP model has high resolution and a nearly isotropic grid (Cuxart et al., 2000). The second parametrisation is the Bougeaul-Lacarrère mixing length (BL89), a non-local turbulent mixing length parametrisation proposed by Bougeault and Lacarrere (1989) that balances the TKE with buoyancy effects to determine the mixing length. This parametrisation is the default mixing length used in the AROME-SWIO model domain. The last parametrisation (DEARDORFF) is the analytical limit of BL89 in a stably stratified atmospheric limit



which corresponds with the results of Deardorff (1980). It was implemented to study the model behaviour in numerical tests. The use of this last parametrisation is discouraged for realistic atmospheric transport.

4 Validation

Validation tests were run using CTL=5, IFINE=5 and LSYNC=300 with output each 30 minutes during a period of 24 hours.

5 The horizontal domain is constrained to one AROME-SWIO gridcell area over land or over sea. The output kernel of FLEXPART, spreading a fraction of particle mass over adjacent horizontal cells, was compensated by adding the output between adjacent cells of FLEXPART-AROME output. The grid cells over land and sea were randomly selected to perform our tests. The cell over land has coordinates 21.1241S 55.3791E, corresponding to a forest area on Reunion island. The cell over sea located at 22.4098S 53.939E, a cell 200 km South-West of the island. The vertical output grid goes up to 5km and is resolved
10 by 100 m thick layers.

4.1 Turbulent conservation of a well-mixed passive tracer

Initially well-mixed passive tracers in position and velocity space should remain unchanged in a turbulent flow. Isolating the vertical turbulence, by setting 3D resolved winds to zero, and using the MDOMAINFILL option to initialise a well-mixed passive tracer, all turbulent modes in FLEXPART-AROME were tested. Accumulation is normalised to the initial mean mixing
15 ratio. By using the MDOMAINFILL option, numerical fluctuations lead to background accumulations and dilution of 3.5% and 4.0% respectively. Results above the sea are shown in fig 4.

The Hanna parametrisation shows systematic accumulation at the surface(11.0%). Modes implemented in FLEXPART-WRF based on TKE violate consistently the well-mixed criterion with turbulent options based on the TKE fields performing worse. Dilution at the surface in TURB_OPTION=2 mode being 46.4% and accumulation at the PBL top 42.3%. The results in
20 TURB_OPTION=3 are slightly better with a maximum dilution of 43.3% near the surface and an accumulation of 31.5% at the PBL top.

The bottom-up configurations perform consistently better than their top-down counterparts. The top-down result with DELTA mixing length has the largest surface accumulation of novel FLEXPART-AROME modes (surface accumulation up to 25.7%). The bottom-up DEARDORFF mode in a step TKE configuration has the least accumulation and dilution of all models (4.3%
25 and 7.4% respectively), however, use of DEARDORFF is not recommended since it is only valid in a stably stratified atmosphere. Modes TURB_OPTION=11 and 111 best conserve the well-mixed state of the passive tracer. With the step TKE performing slightly better in this example (0.9% less dilution and 2% more accumulation) but in tests over land the SDA had better results. (Appendix A)

The remaining accumulation is due to gradients in mixing length. The DELTA mode has smaller L_w near the surface while
30 DEARDORFF has larger mixing lengths at the surface compared to higher altitudes. We see that mass accumulates in these small mixing length regions.

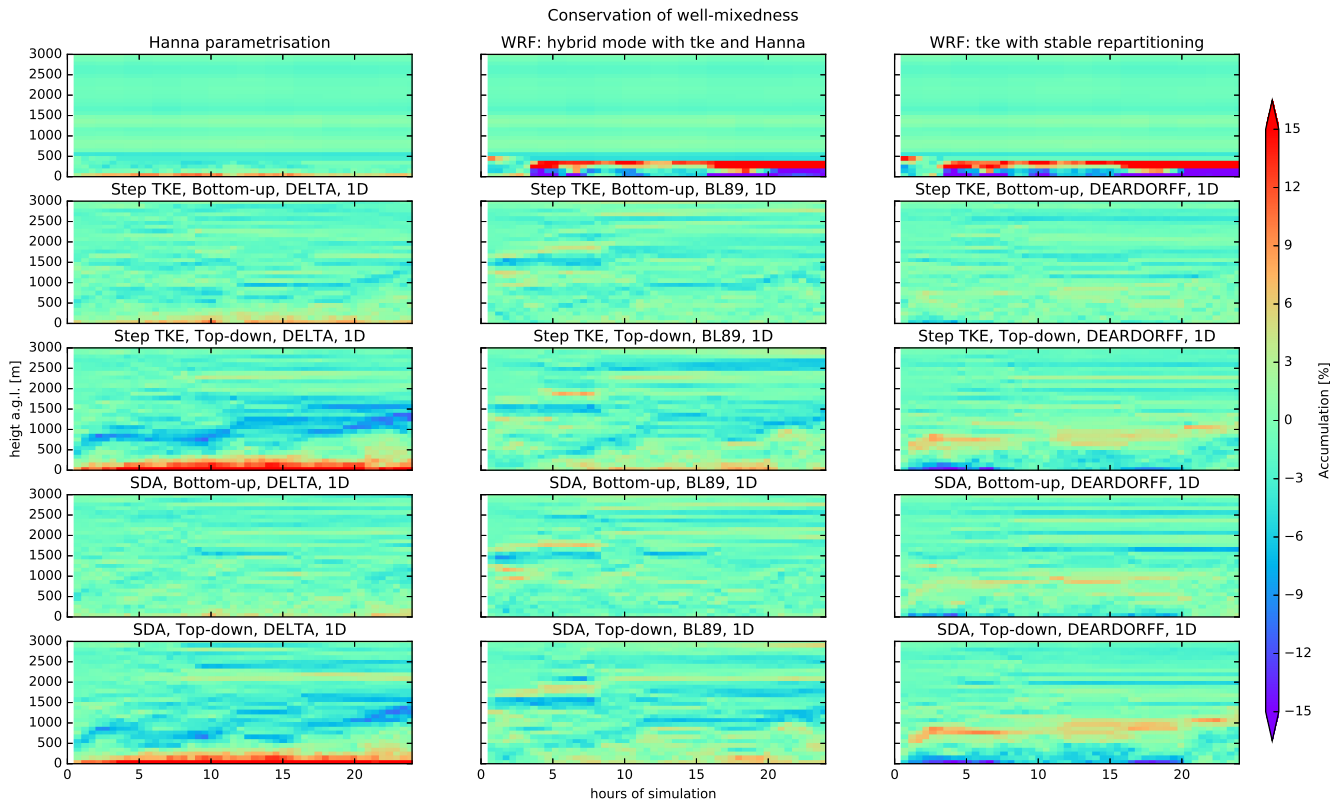


Figure 4. Accumulation in well-mixed test in all different turbulence configurations in FLEXPART-AROME.

4.2 Vertical dispersion of a passive surface tracer in the planetary boundary layer

A point release at the surface at $t=0$ in a FLEXPART-AROME simulation with isolated vertical turbulent motions for different turbulence modes is shown in fig 5.

Concentrations in FLEXPART-WRF turbulent options are larger compared to new modes. Due to shallow convective mixing in new turbulent modes, particles are allowed to breach the PBL top. The tracer is mixed over a larger vertical range causing further dilution not present in FLEXPART-WRF turbulent modes.

There is also limited mixing between turbulent and non-turbulent regions above the shallow convective zone present in the new modes. This in contrast to the sharp PBL in FLEXPART-WRF where all particles are reflected in the isolated turbulence configuration.

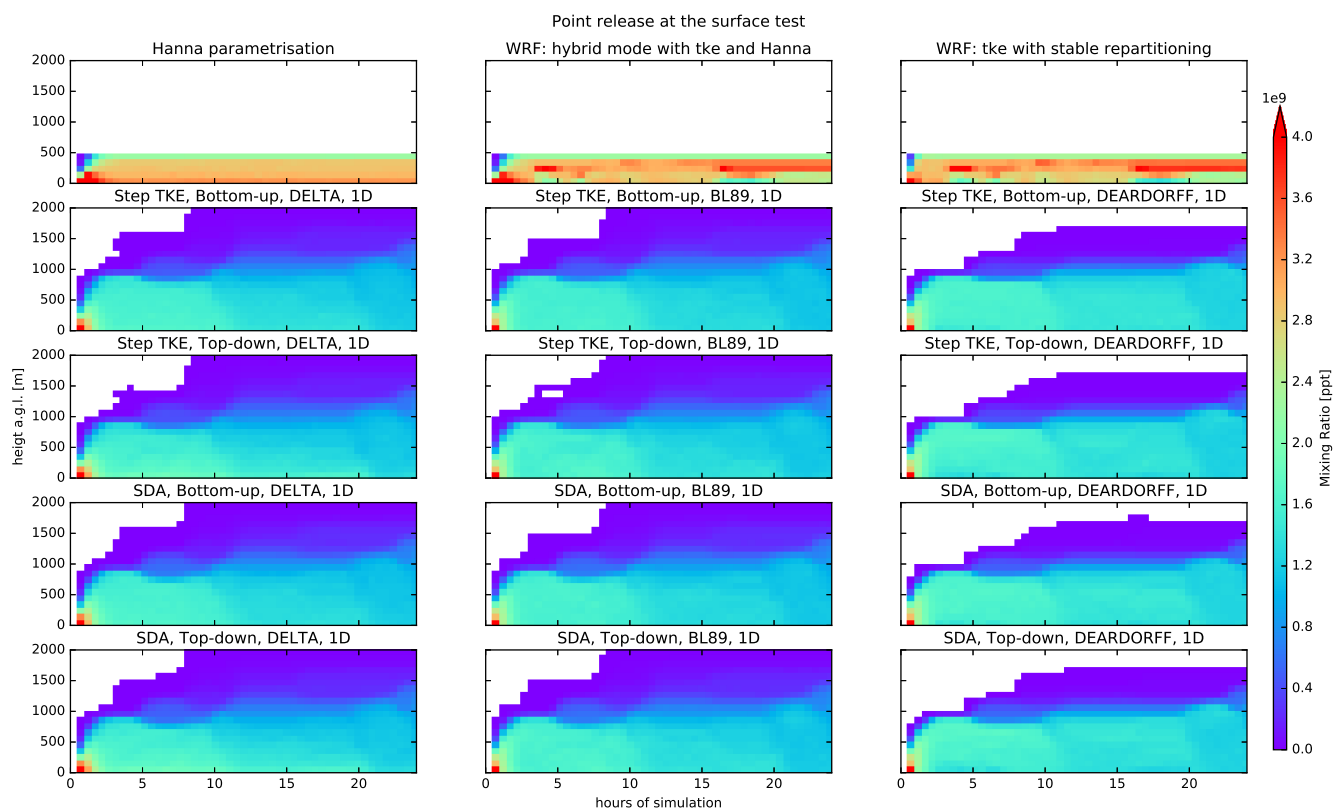


Figure 5. Vertical dispersion of point release at the surface.

5 Performance

5.1 Marine Boundary layer tracer

FLEXPART-AROME was built to simulate particle transport around Reunion Island to analyse measurements at the high altitude Maïdo observatory. To study the marine boundary layer (MBL) impact on measurements taken at the observatory, we continuously release a passive tracer between 0 and 5 meters above the sea with a lifetime of 24 hours. Results shown are after a spin-up time of 24 hours, LSYNC is set to 300, IFINE and CTL equal 5.

Due to the strong coupling of the sea-breeze and up-slope mountainous transport the observatory is located in the MBL during the day while at night the reverse process flushes marine tracers with free-tropospheric air as found in isotopic analysis of water vapor at the Maïdo observatory by Guilpart et al. (2017). Figure 6 shows the MBL tracer at Maïdo using no turbulent motions, Hanna turbulence and the selected new mode, TURB_OPTION=0, 1 and 111 respectively. Differences between modes with turbulence are limited in this example. The passive tracer arrives an hour earlier and has a larger vertical distribution when arriving at the observatory in the new mode compared to the performance of Hanna turbulence.

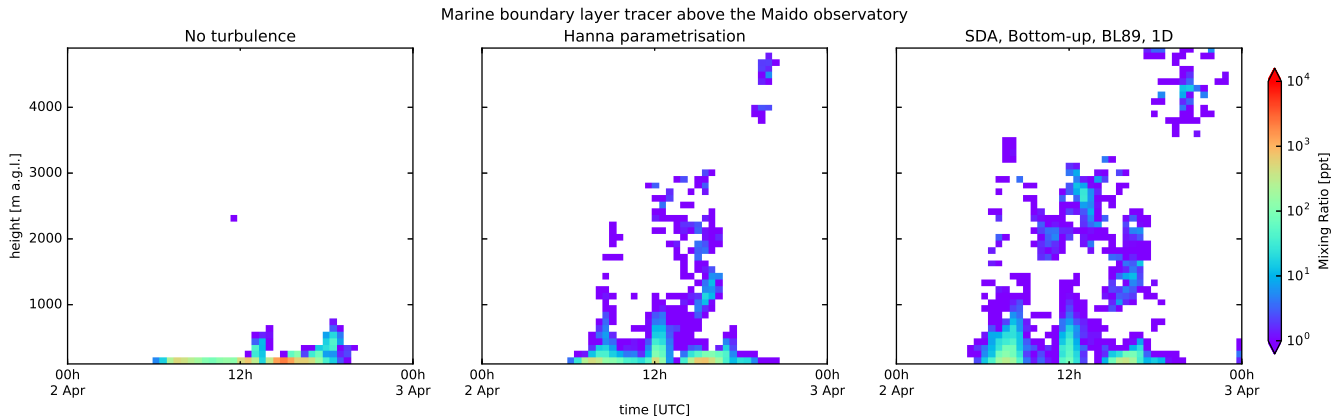


Figure 6. Marine boundary layer tracer profile evolution at the Maïdo observatory. During the day we expect to observe the marine tracer due to efficient coupling of the sea-breeze and up-slope transport while at night the observatory is located in air masses of free tropospheric origin. Although surface mixing ratios can differ between modes, all of the configurations produces the desired diurnal cycle at the observatory on this particular date.

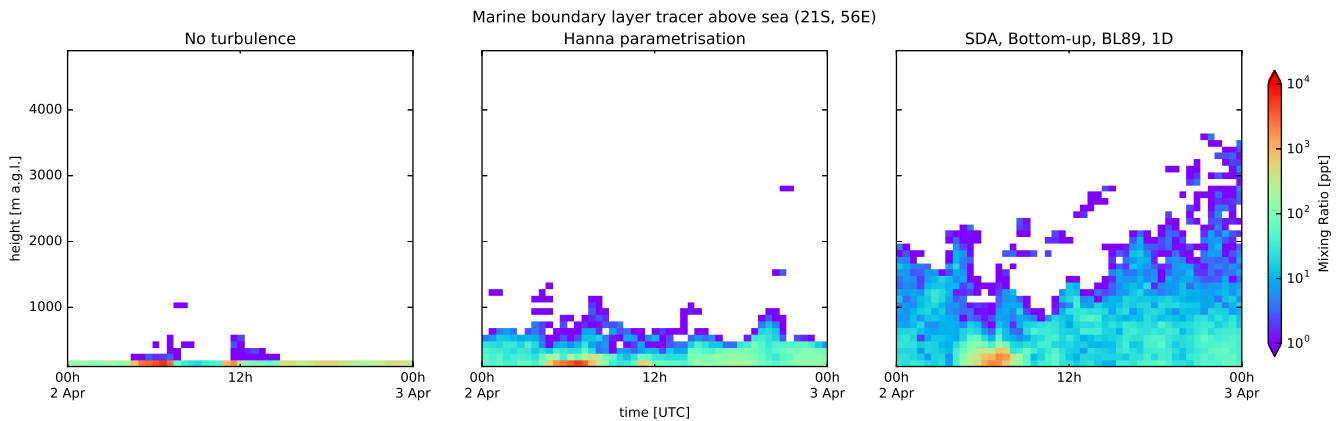


Figure 7. Marine boundary layer tracer profile evolution above sea. We can see that the new turbulent mode mixes the passive tracer up toward higher altitudes due to the turbulent coupling of shallow convection and clouds. This behaviour is not present in the original parametrisation and we only have a shallow boundary layer in which we observe the marine tracer.

Figure 7 shows the marine boundary layer tracer above a random grid cell at sea. In this figure we clearly see the influence of clouds on the dispersion of passive marine tracer in the vertical. Tracers are convected through strong shallow convection in turbulent clouds that are not resolved in the traditional FLEXPART configuration. Surface mixing ratios in the Hanna mode are elevated compared to those obtained with the new turbulent mode as seen in the point release test.

**Table 2.** Computation time ratios relative to the original Hanna parametrisation computation time.

Turbulent configuration		TURB_OPTION	Well-mixed test	Point release test	Marine boundary layer run
No turbulent motion		0	0.96	2.30	1.89
Hanna parametrisation		1	1.00	1.00	1.00
WRF: hybrid mode with TKE and Hanna		2	0.94	1.18	x
WRF: TKE with stable repartitioning		3	1.12	1.32	x
Step TKE	Bottom-up DELTA	10	4.95	1.06	x
	Bottom-up BL89	11	4.89	1.06	x
	Bottom-up DEARDORFF	12	6.81	1.06	x
Step TKE	Top-down DELTA	20	4.95	1.04	x
	Top-down BL89	21	4.99	1.05	x
	Top-down DEARDORFF	22	6.44	1.02	x
SDA	Bottom-up DELTA	110	4.95	1.19	x
	Bottom-up BL89	111	5.21	1.32	1.37
	Bottom-up DEARDORFF	112	9.05	1.24	x
SDA	Top-down DELTA	120	5.20	1.17	x
	Top-down BL89	121	5.58	1.31	x
	Top-down DEARDORFF	122	8.57	1.16	x

5.2 Computation time

Traditionally particles above the PBL are not considered to be turbulent and get advected in one single LSYNC time step. In the new turbulent modes particles above the PBL top are treated in the same way as those below it. This can imply vertical turbulent loops for particles above PBL if the LSYNC input parameter is large. In the well-mixed tests we use the MDOMAINFILL option and initialise a large amount of particles above the PBL. Due to this the relevant novel modes (excluding DEARDORFF) has a mean runtime of 4.8 times that of Hanna. We exclude DEARDORFF in this comparison since its mixing length has no lower limit except the implicit limit imposed by limiting the minimum time step. These modes have a runtime of 7.5 times the Hanna runtime in testing the well-mixedness.

When running the point release the relevant new modes are 15% slower than the original mode. In the marine boundary layer, TURB_OPTION 111 ran 37% longer than the Hanna parametrisation. We also remark that no turbulent parametrisation leads to longer run times in these two tests. This is due to the straightforward implementation of turbulent velocities being set to zero. Time steps in displacing the particle are conserved and since the vertical turbulent dispersion is not represented particles remain in regions with a very low time step. A complete overview of runtimes in reference to the Hanna parametrisation are shown in table 2.



6 Conclusions

We developed the new FLEXPART-AROME limited domain model version of FLEXPART based on FLEXPART-WRF. This configuration was originally build to model transport around Reunion Island in the Indian Ocean, a small volcanic island which has a complex orographic structure, but can be used with any AROME domain. To simulate turbulence as close to the operational meteorological model in the region, we implemented new turbulent modes that ingest TKE fields from the NWP. Due to shallow convection energy being taken into account in determining the 2D TKE fields in AROME, FLEXPART-AROME is able to represent shallow convective behaviour in the atmosphere. Turbulent drift in the model is numerically constrained by using the Thomson interface formalism to conserve the well-mixed state of an initially well-mixed atmosphere. Two possible interpretations of the formalism have been implemented. One approximates turbulence in the FLEXPART-AROME grid by considering every grid-cell to have uniform turbulence with transport being constrained at the vertical boundaries of the model grid. The other uses a so called small discontinuity approximation where the turbulent transport is constrained at each displacement. To better represent the local turbulent state of a particle we also implemented an adaptive vertical time step in turbulent particle transport. This configuration is referred to as a bottom-up approach and performs consistently better in conserving the well-mixed state of the atmosphere compared to the traditional configuration. Three different mixing length parameterisations are implemented: DELTA, BL89 and DEARDORFF. Use of the last parameterisation is discouraged due to it only being valid in stably stratified atmospheres.

New turbulent modes have a computation time that is about 5 times larger compared to the Hanna parameterisation when a large fraction of the particles are above the PBL. However, simulation of tracers predominantly present in the PBL using a new mode in the AROME-SWIO domain only take 15% longer than the original configuration.

FLEXPART-AROME will be used to study the arrival of marine boundary layer tracers at Maïdo observatory on Reunion island, and the vertical distribution of marine aerosols above the ocean in comparison with measurements. Ingestion of meteorological fields coming from the Meso-NH mesoscale research model will also be introduced in the future to simulate transport at higher resolutions around La Réunion to help study air mass transport on a case study basis.

Code availability. The FLEXPART-AROME code is openly accessible on [FLEXPART.eu](https://www.flexpart.eu)

Data availability. Data used for the different tests is available upon request.

Appendix A: Conservations of well-mixedness over land

Shown in figure A1 is the conservation of well-mixedness over land in the morning when the PBL is growing. We see that the DELTA modes all have some accumulation near the surface, the bottom-up SDA mode having the least accumulation, similar to the stable PBL over sea. A surface accumulation over land in Hanna in the bottom layer of maximum 14.5%. Comparing

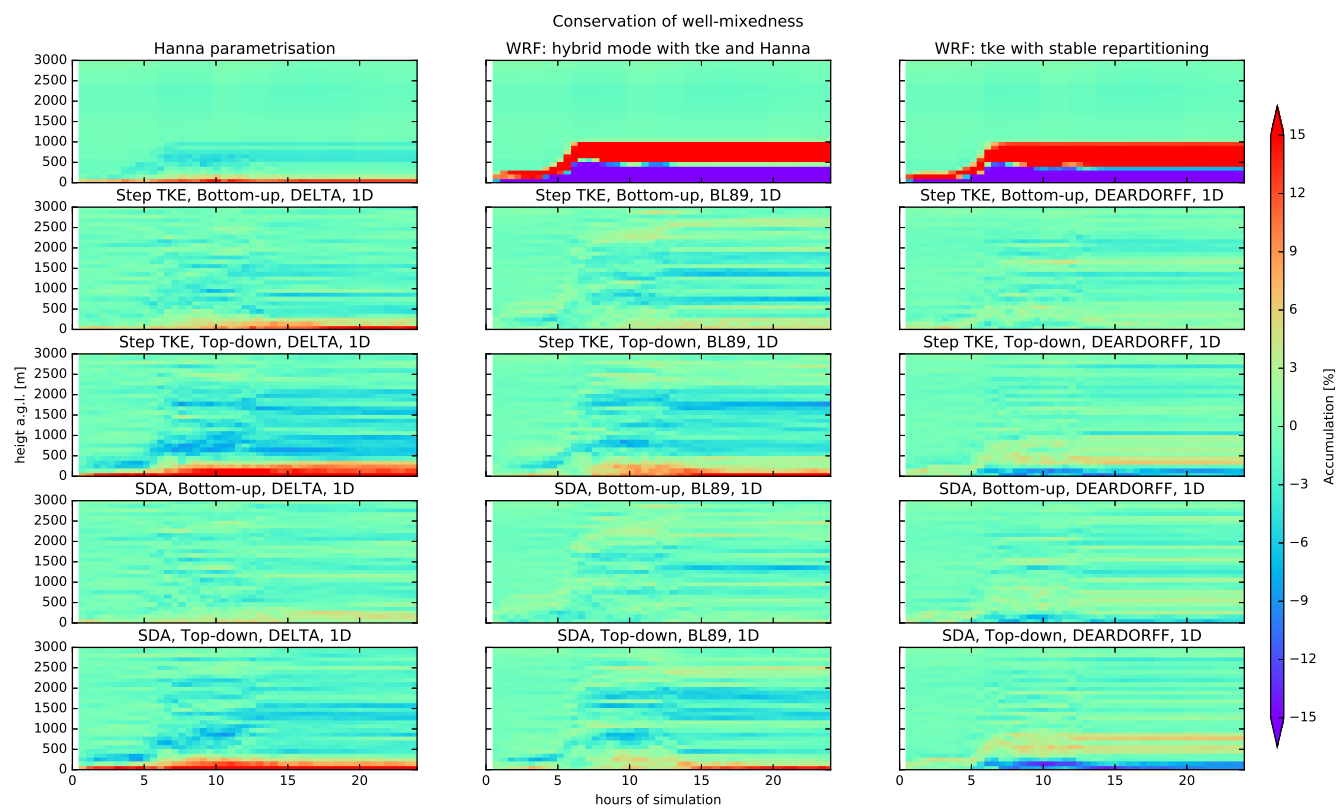


Figure A1. Accumulation in well-mixed test in all different turbulence configurations in FLEXPART-AROME.

the best performing relevant TURB_OPTION parameters 11 and 111 we see that the accumulation in the step TKE mode near the surface is 2.0% larger with the accumulation occurring at the surface from 10 hours simulation onward.

Author contributions. Jérôme Brioude developed the provisional FLEXPART-AROME version and adapted FLEXPART-WRF code to ingest AROME data. He supervised and advised Bert Verreyken who was responsible for implementing and testing the Thomson methodology to use 3D TKE fields in the model. Stéphanie Evan was developer on the FLEXPART-WRF version used as a base and a sought after consultant on development of FLEXPART-AROME.

Competing interests. The authors declare that they have no conflict of interest.



Disclaimer. FLEXPART-AROME is distributed in the hope that it will be useful, but WITHOUT ANY WARRANTY; without even the implied warranty of MERCHANTABILITY or FITNESS FOR A PARTICULAR PURPOSE. See the GNU General Public License for more details.

Acknowledgements. This study has been supported by the project OCTAVE of the "Belgian Research Action through Interdisciplinary Networks" (BRAIN-be) research programme (2017-2021) through the Belgian Science Policy Office (BELSPO) under the contract number BR/175/A2/OCTAVE. We thank Météo France for sharing the AROME output files from forecasts in the South-West Indian Ocean which made this work possible.



References

- Akritidis, D., Zanis, P., Pytharoulis, I., Mavraklis, A., and Karacostas, T.: A deep stratospheric intrusion event down to the Earth's surface of the megacity of Athens, *Meteorology and Atmospheric Physics*, 109, 9–18, <https://doi.org/10.1007/s00703-010-0096-6>, 2012.
- Bertò, A., Buzzi, A., and Zardi, D.: Back-tracking water vapour contributing to a precipitation event over Trentino: a case study, *Meteorologische Zeitschrift*, 13, 189–200, <https://doi.org/10.1127/0941-2948/2004/0013-0189>, <http://dx.doi.org/10.1127/0941-2948/2004/0013-0189>, 2004.
- Bougeault, P. and Lacarrere, P.: Parameterization of Orography-Induced Turbulence in a Mesobeta-Scale Model, *Monthly Weather Review*, 117, 1872–1890, [https://doi.org/10.1175/1520-0493\(1989\)117<1872:POOITI>2.0.CO;2](https://doi.org/10.1175/1520-0493(1989)117<1872:POOITI>2.0.CO;2), [https://doi.org/10.1175/1520-0493\(1989\)117<1872:POOITI>2.0.CO;2](https://doi.org/10.1175/1520-0493(1989)117<1872:POOITI>2.0.CO;2), 1989.
- 10 Brioude, J., Cooper, O. R., Trainer, M., Ryerson, T. B., Holloway, J. S., Baynard, T., Peischl, J., Warneke, C., Neuman, J. A., De Gouw, J., Stohl, A., Eckhardt, S., Frost, G. J., McKeen, S. A., Hsie, E.-Y., Fehsenfeld, F. C., and Nédélec, P.: Mixing between a stratospheric intrusion and a biomass burning plume, *Atmospheric Chemistry and Physics*, 7, 4229–4235, <https://doi.org/10.5194/acp-7-4229-2007>, <https://www.atmos-chem-phys.net/7/4229/2007/>, 2007.
- Brioude, J., Arnold, D., Stohl, A., Cassiani, M., Morton, D., Seibert, P., Angevine, W., Evan, S., Dingwell, A., Fast, J. D., Easter, R. C., 15 Pisso, I., Burkhardt, J., and Wotawa, G.: The Lagrangian particle dispersion model FLEXPART-WRF version 3.1, *Geoscientific Model Development*, 6, 1889–1904, <https://doi.org/10.5194/gmd-6-1889-2013>, <https://www.geosci-model-dev.net/6/1889/2013/>, 2013.
- Cuxart, J., Bougeault, P., and Redelsperger, J.-L.: A turbulence scheme allowing for mesoscale and large-eddy simulations, *Quarterly Journal of the Royal Meteorological Society*, 126, 1–30, <https://doi.org/10.1002/qj.49712656202>, <https://rmets.onlinelibrary.wiley.com/doi/abs/10.1002/qj.49712656202>, 2000.
- 20 D'Auliero, P., Fierli, F., Congeduti, F., and Redaelli, G.: Analysis of water vapor LIDAR measurements during the MAP campaign: evidence of sub-structures of stratospheric intrusions, *Atmospheric Chemistry and Physics*, 5, 1301–1310, <https://doi.org/10.5194/acp-5-1301-2005>, <https://www.atmos-chem-phys.net/5/1301/2005/>, 2005.
- Deardorff, J. W.: Stratocumulus-capped mixed layers derived from a three-dimensional model, *Boundary-Layer Meteorology*, 18, 495–527, <https://doi.org/10.1007/BF00119502>, <https://doi.org/10.1007/BF00119502>, 1980.
- 25 Gentner, D. R., Ford, T. B., Guha, A., Boulanger, K., Brioude, J., Angevine, W. M., de Gouw, J. A., Warneke, C., Gilman, J. B., Ryerson, T. B., Peischl, J., Meinardi, S., Blake, D. R., Atlas, E., Lonneman, W. A., Kleindienst, T. E., Beaver, M. R., Clair, J. M. S., Wennberg, P. O., VandenBoer, T. C., Markovic, M. Z., Murphy, J. G., Harley, R. A., and Goldstein, A. H.: Emissions of organic carbon and methane from petroleum and dairy operations in California's San Joaquin Valley, *Atmospheric Chemistry and Physics*, 14, 4955–4978, <https://doi.org/10.5194/acp-14-4955-2014>, <https://www.atmos-chem-phys.net/14/4955/2014/>, 2014.
- 30 Guilpart, E., Vimeux, F., Evan, S., Brioude, J., Metzger, J.-M., Barthe, C., Risi, C., and Cattani, O.: The isotopic composition of near-surface water vapor at the Maïdo Observatory (Reunion Island, Southwestern Indian Ocean) documents the controls of the humidity of the subtropical troposphere: Water vapor isotopes in Reunion Island, *Journal of Geophysical Research: Atmospheres*, 122, <https://doi.org/10.1002/2017JD026791>, 2017.
- Hanna, S. R.: Applications in Air Pollution Modeling, pp. 275–310, Springer Netherlands, Dordrecht, https://doi.org/10.1007/978-94-010-9112-1_7, 1982.
- 35



- James, R., Bonazzola, M., Legras, B., Surbled, K., and Fueglistaler, S.: Water vapor transport and dehydration above convective outflow during Asian monsoon, *Geophysical Research Letters*, 35, <https://doi.org/10.1029/2008GL035441>, <https://agupubs.onlinelibrary.wiley.com/doi/abs/10.1029/2008GL035441>, 2008.
- Lin, J. C., Gerbig, C., Wofsy, S. C., Andrews, A. E., Daube, B. C., Davis, K. J., and Grainger, C. A.: A near-field tool for simulating the up-
5 stream influence of atmospheric observations: The Stochastic Time-Inverted Lagrangian Transport (STILT) model, *Journal of Geophysical Research: Atmospheres*, 108, 2003.
- MétéoFrance: le modele a maille fine AROME, <http://www.meteofrance.fr/prevoir-le-temps/la-prevision-du-temps/le-modele-a-maille-fine-arome>.
- Pisso, I., Sollum, E., Grythe, H., Kristiansen, N., Cassiani, M., Eckhardt, S., Arnold, D., Morton, D., Thompson, R. L., Groot Zwaafink,
10 C. D., Evangeliou, N., Sodemann, H., Haimberger, L., Henne, S., Brunner, D., Burkhardt, J. F., Fouilloux, A., Brioude, J., Philipp, A., Seibert, P., and Stohl, A.: The Lagrangian particle dispersion model FLEXPART version 10.3, *Geoscientific Model Development Discussions*, 2019, 1–67, <https://doi.org/10.5194/gmd-2018-333>, <https://www.geosci-model-dev-discuss.net/gmd-2018-333/>, 2019.
- Stohl, A.: Operational Emergency Preparedness Modeling—Overview, chap. 22, pp. 266–269, American Geophysical Union (AGU), <https://doi.org/10.1029/2012GM001444>, <https://agupubs.onlinelibrary.wiley.com/doi/abs/10.1029/2012GM001444>, 2013.
- 15 Stohl, A. and Thomson, D. J.: A Density Correction for Lagrangian Particle Dispersion Models, *Boundary-Layer Meteorology*, 90, 155–167, <https://doi.org/10.1023/A:1001741110696>, <https://doi.org/10.1023/A:1001741110696>, 1999.
- Stohl, A., Wotawa, G., Seibert, P., and Kromp-Kolb, H.: Interpolation Errors in Wind Fields as a Function of Spatial and Temporal Resolution and Their Impact on Different Types of Kinematic Trajectories, *Journal of Applied Meteorology*, 34, 2149–2165, [https://doi.org/10.1175/1520-0450\(1995\)034<2149:IEIWFA>2.0.CO;2](https://doi.org/10.1175/1520-0450(1995)034<2149:IEIWFA>2.0.CO;2), [https://doi.org/10.1175/1520-0450\(1995\)034<2149:IEIWFA>2.0.CO;2](https://doi.org/10.1175/1520-0450(1995)034<2149:IEIWFA>2.0.CO;2), 1995.
20
- Stohl, A., Forster, C., Frank, A., Seibert, P., and Wotawa, G.: Technical note: The Lagrangian particle dispersion model FLEXPART version 6.2, *Atmospheric Chemistry and Physics*, 5, 2461–2474, <https://doi.org/10.5194/acp-5-2461-2005>, <https://www.atmos-chem-phys.net/5/2461/2005/>, 2005.
- Thomson, D. J.: Criteria for the selection of stochastic models of particle trajectories in turbulent flows, *Journal of Fluid Mechanics*, 180,
25 529–556, <https://doi.org/10.1017/S0022112087001940>, 1987.
- Thomson, D. J., Physick, W. L., and Maryon, R. H.: Treatment of Interfaces in Random Walk Dispersion Models, *Journal of Applied Meteorology*, 36, 1284–1295, [https://doi.org/10.1175/1520-0450\(1997\)036<1284:TOIRW>2.0.CO;2](https://doi.org/10.1175/1520-0450(1997)036<1284:TOIRW>2.0.CO;2), [https://doi.org/10.1175/1520-0450\(1997\)036<1284:TOIRW>2.0.CO;2](https://doi.org/10.1175/1520-0450(1997)036<1284:TOIRW>2.0.CO;2), 1997.
- Tulet, P., Di Muro, A., Colomb, A., Denjean, C., Dufloy, V., Arellano, S., Foucart, B., Brioude, J., Sellegri, K., Peltier, A., Aiuppa, A., Barthe,
30 C., Bhugwant, C., Bielli, S., Boissier, P., Boudoire, G., Bourriane, T., Brunet, C., Burnet, F., Cammas, J.-P., Gabarrot, F., Galle, B., Giudice, G., Guadagno, C., Jeambly, F., Kowalski, P., Leclair de Bellevue, J., Marquestaut, N., Mékies, D., Metzger, J.-M., Pianezze, J., Portafaix, T., Sciare, J., Tournigand, A., and Villeneuve, N.: First results of the Piton de la Fournaise STRAP 2015 experiment: multidisciplinary tracking of a volcanic gas and aerosol plume, *Atmospheric Chemistry and Physics*, 17, 5355–5378, <https://doi.org/10.5194/acp-17-5355-2017>, <https://www.atmos-chem-phys.net/17/5355/2017/>, 2017.
- 35 Vogelesang, D. H. P. and Holtslag, A. A. M.: Evaluation and model impacts of alternative boundary-layer height formulations, *Boundary-Layer Meteorology*, 81, 245–269, <https://doi.org/10.1007/BF02430331>, 1996.
- Warneke, C., de Gouw, J. A., Del Negro, L., Brioude, J., McKeen, S., Stark, H., Kuster, W. C., Goldan, P. D., Trainer, M., Fehsenfeld, F. C., Wiedinmyer, C., Guenther, A. B., Hansel, A., Wisthaler, A., Atlas, E., Holloway, J. S., Ryerson, T. B., Peischl, J., Huey,



L. G., and Hanks, A. T. C.: Biogenic emission measurement and inventories determination of biogenic emissions in the eastern United States and Texas and comparison with biogenic emission inventories, *Journal of Geophysical Research: Atmospheres*, 115, <https://doi.org/10.1029/2009JD012445>, <https://agupubs.onlinelibrary.wiley.com/doi/abs/10.1029/2009JD012445>.

Zannetti, P.: *Lagrangian Dispersion Models*, pp. 185–222, Springer US, Boston, MA, https://doi.org/10.1007/978-1-4757-4465-1_8, https://doi.org/10.1007/978-1-4757-4465-1_8, 1990.

5 [//doi.org/10.1007/978-1-4757-4465-1_8](https://doi.org/10.1007/978-1-4757-4465-1_8), 1990.